UNIVERSITY OF HELSINKI

https://helda.helsinki.fi

A Structure Function Model Recovers the Many Formulations for Air-Water Gas Transfer Velocity

Katul, Gabriel; Mammarella, Ivan; Grönholm, Tiia; Vesala, Timo

2018-09

American Geophysical Union

http://hdl.handle.net/10138/298625

Katul, G, Mammarella, I, Grönholm, T & Vesala, T 2018, 'A Structure Function Model Recovers the Many Formulations for Air-Water Gas Transfer Velocity', Water Resources Research, vol. 54, no. 9, pp. 5905-5920. https://doi.org/10.1029/2018WR022731

Downloaded from Helda, University of Helsinki institutional repository. https://helda.helsinki.fi

This is an electronic reprint of the original article.

This reprint may differ from the original in pagination and typographic detail.

Please cite the original version.

AGU100 ADVANCING EARTH AND SPACE SCIENCE

Water Resources Research

RESEARCH ARTICLE
10.1029/2018WR022731

A Structure Function Model Recovers the Many Formulations for Air-Water Gas Transfer Velocity

Gabriel Katul[1,2,3,4], Ivan Mammarella[3], Tiia Grönholm[3], and Timo Vesala[3]

[1]Nicholas School of the Environment, Duke University, Durham, NC, USA, [2]Department of Civil and Environmental Engineering, Duke University, Durham, NC, USA, [3]Department of Physics, University of Helsinki, Helsinki, Finland, [4]Karlsruher Institute of Technology, IMK-IFU, Garmisch-Partenkirchen, Germany

Key Points:
- Scaling laws empirically describing gas transfer velocity k_L across marine and coastal systems are theoretically explained
- New theory predicts k_L using Kolmogorov's universal structure function scaling laws for turbulence instead of surface renewal theory
- Work shows how multiple mechanisms with different assumptions subject to eddy-turnover time constraint lead to similar scaling laws for k_L

Correspondence to:
G. Katul,
gaby@duke.edu

Citation:
Katul, G. G., Mammarella, I., Grönholm, T., & Vesala, T. (2018). A structure function model recovers the many formulations for air-water gas transfer velocity. *Water Resources Research*, *54*, 5905–5920. https://doi.org/10.1029/2018WR022731

Received 9 FEB 2018
Accepted 22 JUL 2018
Accepted article online 2 AUG 2018
Published online 3 SEP 2018

Abstract Two ideas regarding the structure of turbulence near a clear air-water interface are used to derive a waterside gas transfer velocity k_L for sparingly and slightly soluble gases. The first is that k_L is proportional to the turnover velocity described by the vertical velocity structure function $D_{ww}(r)$, where r is separation distance between two points. The second is that the scalar exchange between the air-water interface and the waterside turbulence can be suitably described by a length scale proportional to the Batchelor scale $l_B = \eta Sc^{-1/2}$, where Sc is the molecular Schmidt number and η is the Kolmogorov microscale defining the smallest scale of turbulent eddies impacted by fluid viscosity. Using an approximate solution to the von Kármán-Howarth equation predicting $D_{ww}(r)$ in the inertial and viscous regimes, prior formulations for k_L are recovered including (i) $k_L = \sqrt{2/15} Sc^{-1/2} v_K$, v_K is the Kolmogorov velocity defined by the Reynolds number $v_K \eta / \nu = 1$ and ν is the kinematic viscosity of water; (ii) surface divergence formulations; (iii) $k_L \propto Sc^{-1/2} u_*$, where u_* is the waterside friction velocity; (iv) $k_L \propto Sc^{-1/2}\sqrt{g\nu/u_*}$ for Keulegan numbers exceeding a threshold needed for long-wave generation, where the proportionality constant varies with wave age, g is the gravitational acceleration; and (v) $k_L = \sqrt{2/15} Sc^{-1/2} (\nu g \beta_o q_o)^{1/4}$ in free convection, where q_o is the surface heat flux and β_o is the thermal expansion of water. The work demonstrates that the aforementioned k_L formulations can be recovered from a single structure function model derived for locally homogeneous and isotropic turbulence.

Plain Language Summary The problem considered here is a theoretical prediction of mass transfer across and air-water interface. This interfacial transfer phenomenon is featured prominently in global carbon balances, methane, nitrous oxides, dimethyl sulfide, and other gases. It is used to assess the metabolic health of aquatic ecosystems and to determine evasion rates of volatile organic compounds from lakes, estuaries, reservoirs, and large water treatment plants. The novelty of the approach is to link a bulk quantity reflecting the efficiency of swirling motions near the air-water interface to the sizes of eddies and their energetic content responsible for the aforementioned swirling motion. The proposed approach is shown to recover a number of equations describing gas transport across interfaces that summarize a large corpus of experiments and simulations.

1. Introduction

The imprint of air flow over interfaces of water, sand, and snow reflects the transfer of momentum, energy, and matter and has fascinated scientists and general observers alike (Cornish, 1909). The quantitative description of this imprint, especially in the air-water system, soon followed (Rossby & Montgomery, 1935). More recently, the consequences of this imprint on gas exchange between an open water body and the atmosphere is receiving renewed interest given its significance to a plethora of applications. This interfacial transport phenomenon is featured prominently in global balances of carbon dioxide, methane, nitrous oxides, dimethyl sulfide (DMS), and other gases (Bastviken et al., 2011; Bolin, 1960; Butman & Raymond, 2011; Cole et al., 2010; Garbe et al., 2014; Heiskanen et al., 2014; Huotari et al., 2011; Jähne & Haußecker, 1998; Liu et al., 2016; Mammarella et al., 2015; Rantakari et al., 2015; Raymond et al., 2013; Raymond & Cole, 2001; Upstill-Goddard, 2006; Wanninkhof et al., 2009; Wüest & Lorke, 2003). Regionally and locally, gas transport across the air-water interface is used as a water quality index (e.g., dissolved oxygen and aeration rates) and is often needed when determining evasion rates of volatile pollutants from lakes, estuaries, or even large water treatment plants (Chu & Jirka, 2003; Frost & Upstill-Goddard, 1999; Koopmans & Berg, 2015; Liss et al., 2014; Prata et al., 2017). Given their

©2018. American Geophysical Union. All Rights Reserved.

significance to ecosystem metabolism and uncertainty associated with model formulations (Genereux & Hemond, 1992; Marx et al., 2017; Raymond & Cole, 2001), studies on air-water gas transport in streams and rivers are now experiencing a renaissance partly driven by the rapid advancements in miniature eddy-covariance sensors (Berg & Pace, 2017).

Gas fluxes of a slightly or sparingly soluble scalar c across a clear air-water interface are commonly determined from the waterside bulk equation given as

$$F_c = k_L \Delta C, \tag{1}$$

where $\Delta C = C_b - C_s$, C_s is the mean liquid phase saturation concentration at the surface (determined from Henry's law and gas-phase concentration), C_b is the mean concentration of the exchanging gas in the bulk liquid phase, and k_L is the liquid phase mass-transfer velocity (labeled as piston velocity in some literature) describing the turbulent transport efficiency near the interface, the subject here. A large corpus of field and laboratory experiments agree that (Lamont & Scott, 1970; Lorke & Peeters, 2006; Zappa et al., 2007)

$$k_L = \alpha Sc^{-n} v_K, \tag{2}$$

where $v_K = (\nu\epsilon)^{1/4}$ is the Kolmogorov velocity scale formed by the Kolmogorov length $\eta = (\nu^3/\epsilon)^{1/4}$ and time $\tau_k = (\nu/\epsilon)^{1/2}$ scales so as to ensure a Kolmogorov Reynolds number $Re_K = \eta v_K/\nu = 1$ (Pope, 2000; Tennekes & Lumley, 1972), $Sc = \nu/D_m$ is the molecular Schmidt number, ϵ is the mean turbulent kinetic energy (TKE) dissipation rate, ν is the kinematic viscosity, D_m is the molecular diffusivity of scalar c, and $\alpha \approx 0.4$ is a constant determined from experiments (Zappa et al., 2007). Equation (2) appears to hold across a wide range of marine and coastal systems (Zappa et al., 2007) with $\alpha = 0.4$, though variations reported in the literature are by no means small ($\alpha = 0.17 - 0.63$), as discussed elsewhere (Tokoro et al., 2008; Vachon et al., 2010). Some studies amended α with a $\log(\epsilon)$ multiplier or a Reynolds number dependency (Wang et al., 2015), while others suggested that these amendments may be due to changes in exponent n with surface wind conditions (Esters et al., 2017). When the most efficient waterside momentum transporting eddy scales with Kolmogorov variables (labeled as microeddies), then dimensional considerations alone recover equation (2) for $n = 1/2$ without invoking complex transport schemes (Lorke & Peeters, 2006) such as surface renewal (Lamont & Scott, 1970; Soloviev, 2007).

A number of theories and experiments also suggest that the air-water gas transfer velocity is given by (Csanady, 1990)

$$k_L = \beta Sc^{-n} u_*, \tag{3}$$

where u_* is the waterside friction velocity related to the interfacial stress τ_o using $u_*^2 = \tau_o/\rho$, where ρ is the water density. Based on laboratory experiments and comparisons with many data sets, the inferred $\beta \approx 1/16 - 1/9$. Experimental support for equation (3) across a wide range of Sc and u_* has been discussed elsewhere (Hondzo, 1998; Jähne & Haußecker, 1998; Lorke & Peeters, 2006; Prata et al., 2017). Equation (3) has also been derived from two entirely different perspectives. One assumes that equations (2) and (3) are identical (Lorke & Peeters, 2006) depending on the choice of how ϵ is linked to u_* (e.g., law-of-the wall), whereas another assumes equation (3) is linked to moderate wind speed conditions associated with momentum transport by rollers (or circulation zones) on breaking wavelets (Csanady, 1990; Soloviev & Schlüssel, 1994). The mathematical form of equation (3) is also consistent with theories for smooth-wall boundary layers albeit with $n = 2/3$ and $\beta = 0.083$ predicted when assuming a unity *turbulent* Schmidt number (Deacon, 1977). This agreement opened up the possibility of simple transposition of the law-of-the wall derived for smooth solid boundaries to air-water interfaces. Reductions from $n = 2/3$ to $n = 1/2$ (for clear air-water interfaces) are juxtaposition to finite vertical velocity gradients associated with increased surface roughness or mean squared amplitude fluctuations of the water interface (Jähne & Haußecker, 1998). As pointed out elsewhere, the analogy between a solid smooth wall (no slip, $n = 2/3$) and a free surface (finite vertical velocity gradient, $n = 1/2$) cannot be entirely correct (Csanady, 1978; Lamont & Scott, 1970). In fact, finite vertical velocity gradients invited the use of what is termed as *surface divergence* methods. These methods predict (Banerjee et al., 2004)

$$k_L = c_s Sc^{-1/2} \sqrt{\nu \Lambda_o}, \tag{4}$$

where c_s is a similarity constant and Λ_o is the surface divergence of the horizontal velocity components determined from the turbulent vertical velocity w' by

$$\Lambda_o = \sqrt{\overline{\left(\frac{\partial w'}{\partial z}\right)^2}}, \tag{5}$$

for an incompressible flow, where $\partial w'/\partial z$ is to be evaluated at the air-water interface, z is distance from the interface, overline is time averaging, and primes are turbulent fluctuations.

For high wind speeds, the problem becomes far more complicated and general formulations for k_L remain in scarcity and high demand. In such conditions, long surface wave breaking occurs and suppresses the short wavelets, thereby altering the k_L formulation. A surface renewal theory by Soloviev and Schlüssel (1994) based on an assumed log-normal renewal times of eddies predicted that

$$k_L = \gamma Sc^{-1/2} \left(\nu g/u_*\right)^{1/2}, \tag{6}$$

where g is the gravitational acceleration and γ is related to wave age, peak angular frequency of wind waves, and a critical parameter for the onset of wave breaking (Soloviev, 2007; Zhao & Toba, 2001). The log-normal renewal time assumption is now supported by laboratory studies, infrared surface temperature measurements, and Direct Numerical Simulations (DNS) studies (Garbe et al., 2004; Kermani & Shen, 2009; Rao et al., 1971). Interestingly, equation (6) predicts a declining k_L with increasing u_*, which reflects the fact that more of the surface stress is used to support waves instead of waterside turbulence generation. However, if wave breaking that follows enhances ϵ on the waterside, then equation (2) may still provide a realistic estimate of k_L as discussed elsewhere (Kitaigorodskii, 1984). Within the confines of equation (6), the role of bubbles and wave breaking must overcompensate for such decline with increasing u_* if k_L increases beyond its linear value given by equation (3) as reported by experiments (Jähne & Haußecker, 1998). Wave breaking leads to a cascade of other events such as bubble-mediated transfer of scalars where Henry's law must also be amended when determining C_s. These amendments, which also vary with wind speed, surfactants, and water temperature, have been discussed elsewhere (Memery & Merlivat, 1985; Woolf & Thorpe, 1991) and their effects on k_L are not considered. Notwithstanding these limitations, few field experiments used DMS to explore the k_L dependency on mean wind speed at 10 m above the air-water interface (U_{10}). DMS is not impacted by bubble-mediated transfer and is thus an ideal tracer for exploring k_L in the absence of bubbles at high U_{10}. Few experiments support the decline of k_L for DMS with increasing U_{10} (Bell et al., 2013, 2017; Huebert et al., 2004), while others do not offer such strong evidence (Bigdeli et al., 2018). Some laboratory studies suggest a saturation behavior of k_L with u_* at very high u_* (Komori et al., 1993; Vlahos & Monahan, 2009).

The goal here is *not* to propose a new formulation for k_L or compare various k_L formulations with data. Instead, a new interpretation rooted in a link between k_L and the spectral shape of turbulence is proposed without resorting to surface renewal schemes. This link assumes that k_L is a scale-dependent turnover velocity (instead of a piston velocity) and all the aforementioned formulations reviewed here (including their associated constants) reflect different scales over which the spectrum is integrated (Katul & Liu, 2017a). Hence, all the aforementioned k_L formulations maybe recovered from an accepted structure function shape describing turbulence at high Reynolds numbers on the waterside. In essence, the interpretation of k_L proposed here (in the absence of waves or wavelets) is shown to be a hybrid between the original theory proposed by Lamont and Scott (1970) and the dimensional considerations of Lorke and Peeters (2006). It maintains the spectral energetic content in eddies originally employed by Lamont and Scott (1970) but without utilizing surface renewal schemes. However, the effective eddy size over which the energy content is being evaluated is derived from dimensional considerations analogous to those used by Lorke and Peeters (2006). When small wavelets or waves are present, the choices of these length scales are determined entirely from plausibility considerations and ad hoc arguments. Nonetheless, by showing connections between established k_L formulations and the structure function for vertical velocity, the work here offers a different perspective about links between eddy sizes, their energetics, and k_L beyond surface renewal theory. Also, it allows for a single expression to be derived that interpolates between all the aforementioned prior formulations. Last, it is envisaged that progress in this area can contribute to analogous problems in surface hydrology such as water vapor transfer from rough surfaces into a turbulent atmosphere as may occur during evaporation from bare soil or vegetated systems (Brutsaert, 1975; Haghighi & Or, 2013; Katul & Liu, 2017b; Shahraeeni et al., 2012).

2. Theory

2.1. Background and Definitions

For slightly and sparingly soluble gases, the small D_m implies that the resistance to mass transfer in air is negligible compared to its water counterpart (Bolin, 1960). It is well known that when $Sc >> 1$, scalar transport near

interfaces is assumed to be conducted by eddies commensurate in size to the Batchelor scale $l_B = Sc^{-1/2}\eta$ (Batchelor, 1959; Hill, 1978; Lorke & Peeters, 2006). The l_B is viewed as the smallest length scales of turbulent tracer fluctuations. This length scale can be derived in multiple ways—but the textbook versions associate this length scale to controls over a diffusive time scale t_m characterizing a diffusive length scale $l_D = \sqrt{D_m t_m}$. When $Sc >> 1$, then water viscosity restricts t_m and t_m is given by τ_k resulting in

$$l_D \propto \sqrt{\left(\frac{\nu}{Sc}\right)\left(\frac{\nu}{\epsilon}\right)^{1/2}}, \tag{7}$$

thereby recovering $l_D = l_B = Sc^{-1/2}\eta$. With this background, and based on dimensional considerations alone, Lorke and Peeters (2006; hereafter referred to as LP06) showed that for $Sc >> 1$, the viscous sublayer thickness ($\delta_V \propto \nu/u_*$) exceeds that of the molecular diffusive layer of scalar c ($\delta_D \propto D_m/u_*$) and the Batchelor scaling restricts the path length over which scalar transport must occur. Hence, $k_L \propto D_m/\min\left(\delta_V, \delta_D\right)$. Because $\delta_V > \delta_D$, k_L is dominated by concentration differences along δ_D and $k_L \sim D_m/\delta_D$. This result is virtually identical to the classical thin-film theory (Fortescue & Pearson, 1967; Lewis & Whitman, 1924). With $\delta_D \propto l_B$,

$$k_L \propto \frac{D_m}{\delta_D} = \frac{\nu Sc^{-1}}{Sc^{-1/2}\left(\nu^3/\epsilon\right)^{1/4}} = \frac{Sc^{-1/2}}{\nu^{-1}\nu^{3/4}\left(\epsilon\right)^{-1/4}}, \tag{8}$$

thereby recovering equation (2). LP06 also provides some arguments about expected sizes of $\delta_D = 2\pi l_B$ and $\delta_V = 8.6\nu/u_*$ based on what is known about variations in turbulent statistics (eddy diffusivity) in the viscous (and buffer) regions of wall-bounded flows.

2.2. Surface Renewal Schemes: Large- and Micro-Eddy Models

In air-water mass-transfer studies, several limitations of classical thin-film theory have been addressed via surface renewal schemes. Surface renewals are viewed as approximations to upwellings of eddies in which water flows toward the interface and is then deflected parallel to the interface. As these elements deflect by the air-water surface, flow occurs along the surface leading to a finite $\partial u/\partial x + \partial v/\partial y$ and subsequently plunges back into the body of the water. Here u and v are the velocity components along the longitudinal (or x) and lateral (or y) directions, respectively. Fresh water elements are then transported very close to the surface so that mass is only transferred by molecular diffusion at the surface. The assumption of instantaneous water element transport, often invoked in surface renewal analysis, is hydrodynamically unrealistic but corrections to it do not alter much gas transfer velocity formulations. Eddies associated with upwellings and contact with the interface are effective in mass transfer across an interface as shown using conditional sampling methods (Komori et al., 1990). Near an air-water interface, DNS also reveal a rich turbulent regime where inertial, pressure, and viscous coupling all play a role (Herlina & Wissink, 2014). Likewise, rapidly acquired thermal infrared images suggest that thermal signatures of the contact durations of eddies with the air-water interface follows a log-normal distribution in agreement with a number of fully developed turbulence theories (Garbe et al., 2004). Hence, the main difference between wall-bounded flow and flow near air-water interfaces is the flow pattern associated with upwelling events close to the surface. In the case of wall-bounded flows, the boundary conditions on this flow are $w = 0$ and $\partial w/\partial z = 0$ resulting in $\partial u/\partial x + \partial v/\partial y = 0$ (no surface divergence). For those boundary conditions, the viscous sublayer cannot be readily penetrated by eddies. In the case of air-water interface, $w = 0$ but $\partial w/\partial z$ is finite (and large) at the interface. Laboratory experiment measuring the waterside $w(z)$ at a small distance away from the air-water interface and $\partial u/\partial x + \partial v/\partial y$ at the interface suggest that (Brumley & Jirka, 1987)

$$w(z) = -\left(\frac{\partial u}{\partial x} + \frac{\partial v}{\partial y}\right)_{z=0} z^*, \tag{9}$$

where z^* was shown to be commensurate with η, though by no means this view is widely accepted and larger eddies have been postulated to impact $w(z)$.

As discussed elsewhere (Katul & Liu, 2017a, 2017b; Komori et al., 1990), surface renewal theory predicts

$$k_L \propto \sqrt{D_m \frac{\sigma_t}{L_I}}, \tag{10}$$

where σ_t is a characteristic turbulent velocity and L_I is a length scale describing the upwelling eddy sizes penetrating the viscous sublayer and efficiently exchanging mass with the air-water interface via molecular

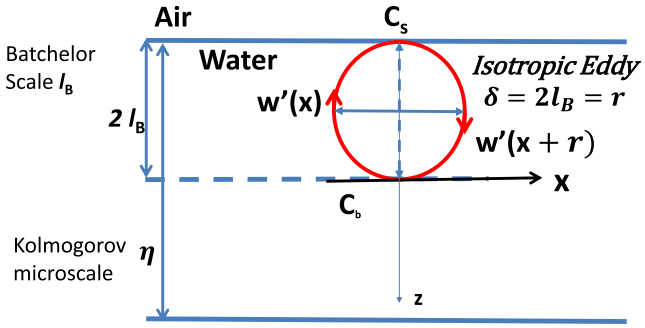

Figure 1. The Kolomogorov microscale η and the Batchelor scale l_B for $S_c >> 1$ below the air-water interface. Microeddies are assumed to be isotropic of size r moving scalars to and from the interface from regions with constant concentration C_b (labeled as bulk region) to the surface characterized by an interface concentration C_s. The turnover velocity is defined by the magnitude of the relative velocity difference between two points $|\Delta w'(r)| = |w'(x+r) - w'(x)| = \sqrt{D_{ww}(r)}$ separated by $r = 2l_B$ as shown. The $k_L = \sqrt{D_{ww}(r)}$.

diffusion. Two types of models have been proposed to estimate σ_t and L_I: the so-called microeddy approach (Lamont & Scott, 1970) and the energy-containing eddy approach (Fortescue & Pearson, 1967; Komori et al., 1990). Unlike wall-bounded surfaces, the air-water interface allow eddies of various sizes to make contact with the interface for finite durations (the basis of surface renewal). The problem then is what type of eddies dictate the values of σ_t and L_I? In the energy-containing eddy approach, $\sigma_t \propto \sqrt{e_{tke}}$, where e_{tke} is the TKE and L_I is the integral length scale of the flow away from the interface. In the microeddy approach, these velocity and length scales are given by their Kolmogorov values ($\sigma_t = v_K$ and $L_I = \eta$), thereby recovering equation (2) with $n = 1/2$. As a bridge between the microeddy and energetic-eddy approaches, a Reynolds number $Re_t = \sigma_t L_I/\nu >> 1$ is first defined to ensure a turbulent state at the macroscopic level near the interface. Next, it is assumed that the bulk TKE dissipation $\epsilon \propto \sigma_t^3/L_I$, thereby resulting in $\eta/L_I \propto Re_t^{-3/4}$, or $L_I \propto Re_t^{3/4}\eta$ (Fortescue & Pearson, 1967; Tennekes & Lumley, 1972). Replacing these estimates in equation (10), the energy-containing eddy approach yields

$$k_L \propto Re_t^{-1/4}\left[Sc^{-1/2}v_K\right]. \tag{11}$$

This result is analogous to equation (2) (i.e., the microeddy approach) but with α decreasing as $Re_t^{-1/4}$ with increasing Re_t. DNS and experimental support (laboratory and field) for this finding are discussed elsewhere (Herlina & Wissink, 2014; Komori et al., 1990; Wang et al., 2015), at least for moderate Re_t. Clearly, in the limit of very large Re_t, k_L may become unrealistically small suggestive that α must become independent of Re_t. The independence of α from Re_t is analogous to how the Darcy-Weisbach friction-factor becomes independent from the bulk Reynolds number at very high bulk Reynolds numbers in pipe and open channel flows. A number of studies demonstrated that α becomes constant independent of Re_t for very large Re_t (i.e., consistent with the microeddy approach) but depends on $Re_t^{-1/4}$ for moderate Re_t (Theofanous et al., 1976; i.e., consistent with the energetic-eddy approach). Using laboratory experiments and DNS, the crossover between these two mass-transfer regimes (i.e., energetic eddy to microeddy) was determined to be around $Re_t \approx 500$ (Herlina & Wissink, 2014; Theofanous et al., 1976). In fact, the DNS results visually reveal large-eddy penetration up to the interface of near-isotropic eddies originating from the bulk fluid at moderate $Re_t < 500$ and across a wide range of Sc values. Also, the same DNS and laboratory studies confirm the $Sc^{-1/2}$ scaling in equation (11), at least for clear interfaces. For the microeddy approach, surface tension effects (or the Weber number) are no longer relevant to k_L formulations.

2.3. The Structure Function Approach

Noting that F_c is related to the waterside mean concentration difference between the air-water interface and the bulk layer at some δ below the water surface, then $F_c = w_{TO}\Delta C$ and k_L is interpreted as an effective turnover turbulent velocity $|w_{TO}|$ instead of a piston velocity (Katul & Liu, 2017a) as shown in Figure 1.

The magnitude of this velocity is $\sqrt{w_{TO}^2}$, where w_{TO}^2 is the mean squared vertical velocity of eddies of size $r = \delta$ given by

$$w^2{}_{TO} = \overline{[w'(x+r) - w'(x)]^2} = D_{ww}(r), \tag{12}$$

where w' is the turbulent vertical velocity as before, x is an arbitrary position, r is separation distance assumed to represent mean eddy sizes, and $D_{ww}(r)$ is the second-order structure function of the turbulent vertical velocity. The large Sc assumption implies that as eddies turn fluid elements, the loss of scalar mass by molecular diffusion from those fluid elements can be ignored over the smallest time scales commensurate with τ_K. The inference of w_{TO}^2 may be achieved via the scale-wise integration of the spectrum of w' ($E_{ww}(k)$, k is wavenumber). However, the physical space or structure function representation for $|w_{TO}|$ is preferred for two reasons: (1) The structure function already integrates spectral energy content across scales—as given by the approximate expression (Davidson, 2015; Katul et al., 2016)

$$r\frac{dD_{ww}(r)}{dr} \sim kE_{ww}(k), \tag{13}$$

and (2) at $r = 0$ and as $r \to \infty$, the bounds on the structure function are unambiguous and given by $D_{ww}(0) = 0$ and $D_{ww}(\infty) \to 2\sigma_w^2$, where $\sigma_w = \sqrt{\overline{w'^2}}$ is the vertical velocity standard deviation. For $E_{ww}(k)$, how those bounds are approached is more problematic. In the case of nonflat water surfaces associated with equations (6) and (3), the choice t_m must be viewed as ad hoc but plausible. The simplest model for $D_{ww}(r)$ is the Kolmogorov inertial subrange scaling (or K41) for locally homogeneous and isotropic turbulence (Kolmogorov, 1941) adjusted by a viscous cutoff given by

$$\frac{D_{ww}(r)}{C_o(\epsilon r)^{2/3}} = 1 - \frac{1}{\zeta}\mathrm{Daw}_F(\zeta), \tag{14}$$

where C_o is the Kolmogorov constant, $\zeta = \theta(r/\eta)^{2/3}$, $\theta = (10C_o)^{-1/2}$, and the Dawson function is given by

$$\mathrm{Daw}_F(\zeta) = \exp(-\zeta^2)\int_0^{\zeta}\exp(p^2)dp \approx \zeta - \frac{2}{3}\zeta^3 + \cdots. \tag{15}$$

This expression is an approximate solution to the von Kármán-Howarth equation (von Kármán & Howarth, 1938) derived elsewhere (Katul et al., 2015). When this expression is converted to the spectral domain, it recovers the spectral *bottleneck* reported at the crossover from inertial to dissipation (Katul et al., 2015). This bottleneck is commonly identified by a bump when the compensated spectrum $k^{5/3}E_{ww}(k)$ is plotted against k in the vicinity of $k\eta \approx 0.1$ and has been the subject of active research (Davidson, 2015; Dobler et al., 2003; Donzis & Sreenivasan, 2010; Frisch et al., 2013, 2008; Herring et al., 1982; Hill, 1978; Katul et al., 2015; Meyers & Meneveau, 2008). The assumed spectrum by Lamont and Scott (1970) exhibits an inertial subrange adjusted with a power-law viscous cutoff based on the Kovasznay spectrum. Such a spectrum does not exhibit any bottlenecks, which is not consistent with DNS (Meyers & Meneveau, 2008) or high Reynolds number laboratory experiments (Saddoughi & Veeravalli, 1994). As earlier noted, $k_L = \sqrt{D_{ww}(r)}$ and $D_{ww}(r)$ depend on the scale-wise integrated spectrum in equation (13); hence, not all spectral features are required to reproduce $D_{ww}(r)$ from $E_{ww}(k)$. That is, despite the shortcoming of the spectral shape for $E_{ww}(k)$ used by Lamont and Scott (1970), the outcome for k_L may be reasonably insensitive to the presence of the aforementioned bottleneck. For $r/\eta >> 10$, $D_{ww}(r) = C_o(\epsilon r)^{2/3}$ and the effects of viscous cutoff on $D_{ww}(r)$ can be ignored. However, the majority of conditions to be considered here deal with cases where the viscous effects on $D_{ww}(r)$ are significant (at least in the microeddy dominated Re_t). Setting $r = 2(D_m t_m)^{1/2} = 2(\nu Sc^{-1} t_m)^{1/2}$ (instead of l_B) and considering only the two-term expansion of the Dawson function yields

$$D_{ww}(r) = w_{TO}^2 = \frac{2}{15}Sc^{-1}(\epsilon t_m), \tag{16}$$

where the factor 2 is discussed in Appendix A as well as further rationale for selecting the Batchelor scale for r (in the microeddy regime where $Re_t >> 500$). The linearity in ϵt_m here bares resemblance to the Lagrangian structure function in the inertial subrange (Monin & Yaglom, 1975; Ouellette et al., 2006; Yeung, 2002) but with two exceptions: (1) the constant 2/15 is independent of the Kolmogorov constant, and (2) the dependency of k_L^2 on Sc^{-1} arises because scalar molecular diffusion dictates the effective eddy sizes transporting scalar c. The derivation of equation (16) also makes no specific assumption about the boundary conditions (e.g., the law-of-the wall). In fact, the structure function shape assumed here applies universally to all locally homogeneous and isotropic turbulence, which is appropriate for eddy sizes much smaller than the integral length scale of the flow (i.e., microeddies). The indirect effect of such boundary conditions will be incorporated into models of ϵ and estimates of t_m.

The predicted $k_L \sim Sc^{-1/2}$ is consistent with all prior surface renewal theories and surface divergence arguments. In essence, assuming a $k_L = \sqrt{D_{ww}(r)}$ implies a finite $|dw'/dz| \sim \sqrt{\overline{[w'(z+r) - w'(z)]^2}}/r$ at $r \sim l_B$ near the interface ($z \to 0$). It has been shown theoretically (Csanady, 1990; Hasse, 1980; Lamont & Scott, 1970), experimentally (Hondzo, 1998; Jähne & Haußecker, 1998), and using DNS (Fredriksson et al., 2016; Takagaki et al., 2016) that a finite dw/dz at the interface is responsible for $k_L \sim Sc^{-1/2}$, whereas a $dw/dz = 0$ invariably leads to a $k_L \sim Sc^{-2/3}$. The $k_L \sim Sc^{-1/2}$ is sufficiently prevalent for clear air-water interfaces that when relating k_L across different gases or conditions (e.g., $Sc = 600$) or when inferring k_L from surface temperature measurements, conventional practice is to set $n = 1/2$ not 2/3 (Asher et al., 2004; Csanady, 1990; Jähne & Haußecker, 1998). An obvious critique here that also applies to surface renewal, eddy penetration, and surface divergence theories (Csanady, 1990) is the absence of a rigorous link between molecular diffusion at the water surface and eddy transport below the water surface. The structure function approach simply packs them into l_B.

Notwithstanding this critique, it is shown next that the multiple formulations for k_L reviewed in section 1 can be recovered with appropriate choices of t_m and models for ϵ where needed (instead of σ_t and L_I in the surface renewal formation of equation (10). The simplest model for ϵ may be derived from an idealized stationary and planar-homogeneous TKE budget with no mean vertical velocity where production and dissipation rates of TKE are in balance. For this idealized state,

$$\epsilon = -\overline{u'w'}\frac{dU}{dz} + \beta_o g q_o = u_*^2 \frac{dU}{dz}\left(1 - Ri_f\right); Ri_f = \frac{\beta_o g q_o}{\overline{u'w'}(dU/dz)}; u_*^2 = -\overline{u'w'} = \frac{\tau_o}{\rho}, \tag{17}$$

where dU/dz is the waterside mean velocity gradient, β_o is the thermal expansion coefficient of water that varies with absolute water temperature T, Ri_f is a flux Richardson number, and q_o is the surface kinematic vertical heat flux (positive upward) assumed to be the main mechanism responsible for buoyancy generation or destruction of TKE (i.e., salinity effects or air entrainment on the water density gradients are ignored). Stable and unstable stratification occur when $q_o < 0$ (downward heat flux, $Ri_f > 0$) and $q_o > 0$ (upward heat flux, $Ri_f < 0$), respectively. The two generic terms (mechanical production and buoyant production/dissipation) impacting ϵ appear to be sufficient to recover a wide range of field conditions as discussed elsewhere (MacIntyre et al., 2010; Tedford et al., 2014). In stable stratification, an $\epsilon > 0$ (i.e., turbulence is still active) requires $0 < Ri_f < 1$, though a maximum value of about $Ri_{f,max} = 0.2 - 0.25$ has been derived that ensures well-developed turbulence and K41 scaling to hold (Katul et al., 2014; Li et al., 2015). However, the $Ri_{f,max} = 0.2 - 0.25$ is not connected with laminarization of the flow (Galperin et al., 2007; Grachev et al., 2013; Li et al., 2016; Zilitinkevich et al., 2008). The q_o may be inferred as a residual of the air-side energy balance considerations. It is the outcome of an imbalance between the net long-wave radiation at the interface and the sum of sensible and latent heat fluxes into the atmosphere. The effects of shortwave radiation are ignored if its attenuation in water over a small distance $\sim 2l_B$ is small. In what follows, it is assumed that $|Ri_f| << 1$ for the estimation of ϵ and dU/dz unless stated otherwise. This assumption is mainly employed for comparisons with laboratory studies and published expressions in nonstratified conditions. The expected effects of Ri_f on k_L are discussed separately. It is worth noting that DNS and numerous experiments on smooth-wall boundary layers (with $|Ri_f| << 1$) suggest that TKE production and dissipation near the wall are not in balance and production may exceed dissipation by a factor of 1.7 (McColl et al., 2016; Pope, 2000). This imbalance has obvious consequences on equation (17) but not appreciably on k_L. A $k_L \sim \epsilon^{1/4}$ means that a factor of 1.7 in dissipation rate overestimate from TKE production translates to a factor of 1.14 adjustment to k_L. Before linking models of k_L with u_*, the case where k_L varies with ϵ only is first considered.

2.4. Recovering $k_L = \alpha Sc^{-1/2}(\nu\epsilon)^{1/4}$ (Abstract, i and v)

This k_L formulation is directly recovered when setting $t_m = \tau_K$. That is,

$$k_L = |w_{TO}| = \sqrt{\frac{2}{15}} Sc^{-1/2} \sqrt{\left[\epsilon\left(\frac{\nu}{\epsilon}\right)^{1/2}\right]} = \sqrt{\frac{2}{15}} Sc^{-1/2}(\nu\epsilon)^{1/4}. \tag{18}$$

The finding that $k_L \sim Sc^{-1/2}(\nu\epsilon)^{1/4}$ has been discussed elsewhere (Katul & Liu, 2017a). However, the analysis here goes further by proposing $\alpha = \sqrt{2/15} = 0.37$, which is reasonably close to the value $\alpha = 0.42$ reported by Zappa et al. (2007) and, more recently, by Esters et al. (2017) for open ocean when setting $n = 1/2$. Another multisite study reported a $0.39 < \alpha < 0.43$ (Vachon et al., 2010) and noted the sensitivity of their inferred α to the method and depth used when estimating ϵ. Also, the predicted α here agrees with recent DNS analysis (Fredriksson et al., 2016) estimating an $\alpha = 0.39$ for the free slip case at the air-water interface. The original work of Lamont and Scott (1970) also reported an $\alpha = 0.4$. Kitaigorodskii (1984) derived equation (18) for temperature (without the constant $\sqrt{2/15}$) and further proposed that it is applicable for wavy surfaces experiencing wave breaking. The wave-breaking component primarily impacts ϵ, not the gas transfer law for k_L, a point to be discussed later on.

As a bridge to the energetic-eddy hypothesis for moderate Re_t, it is worth noting that equation (16) can directly recover the α dependency on Re_t. The ratio of the turnover time scale of large eddies ($=L_I/\sigma_t$) to microeddies ($=\tau_K$) is $\sim Re_t^{1/2}$ (Tennekes & Lumley, 1972). Setting $t_m = \tau_K Re_t^{1/2}$ (i.e., large-eddy formulation) instead of $t_m = \tau_K$ (microeddy formulation) yields $k_L \sim S_c^{-1/2}\sqrt{\epsilon\tau_K Re_t^{1/2}}$. That is, k_L from a microeddy formulation is reduced below the k_L arising from energetic-eddy considerations by a factor of $Re_t^{1/4}$. The subunity dependence on Re_t by k_L means that when Re_t increases from 100 to 10,000, alterations in k_L are about a factor of 3.

In the limit of large $-Ri_f$ (i.e., approaching free convection limit), the above expression yields

$$k_L = \sqrt{\frac{2}{15}} Sc^{-1/2} \left(\nu g \beta_o q_o\right)^{1/4}, \tag{19}$$

which can be expressed in dimensionless numbers as

$$k_L = \sqrt{\frac{2}{15}} Sc^{-1/2} Pr^{1/2} Ra^{1/4} \frac{\nu}{h_c}, \tag{20}$$

where $Pr = \nu/\alpha_T$ is the molecular Prandtl number, α_T is the molecular diffusivity of heat in water, and h_c is the thickness of the convective layer derived from a constant $q_o \propto \Delta T/h_c$, where ΔT is the temperature difference between the surface and the waterside well-mixed layer, and $Ra = (h_c^3)(g\beta_o)(\Delta T)/(\nu\alpha_T)$ is the Rayleigh number. Equation (19) agrees with predictions from a surface renewal model (Soloviev & Schlüssel, 1994) that assumes the mean renewal time is proportional to $\nu(\alpha_T g q_o)^{-1/2}$ (Foster, 1971). Moreover, equation (19) is in agreement with DNS runs (Fredriksson et al., 2016) that reported an expression, given by

$$k_L = 0.39 Sc^{-1/2} \left(\nu \beta_o g q_o\right)^{1/4}, \tag{21}$$

that fits their free convective runs.

2.5. Recovering the Surface Divergence Formulation (Abstract, ii)

Recovering equation (4) from (18) can be readily achieved for isotropic turbulence when noting that (Tennekes & Lumley, 1972)

$$\epsilon = 15\nu \overline{\left(\frac{\partial w'}{\partial z}\right)^2}. \tag{22}$$

Inserting equation (22) into (18) leads to

$$k_L = \frac{\sqrt{2}}{15^{1/4}} Sc^{-1/2} \sqrt{\nu \Lambda_o}, \tag{23}$$

which is identical to equation (4) when $c_s = \sqrt{2}/(15^{1/4}) \approx 0.7$. This estimate is in acceptable agreement with the recent DNS studies reported by Fredriksson et al. (2016), where $c_s = 0.57$ was determined from fitting to DNS using surface state variables. It also agrees with estimates by Ledwell (1984) who reported $c_s = 0.64$ and by McCready et al. (1986) who reported $c_s = 0.71$.

In what follows, the $k_L = \left[D_{ww}(r)\right]^{1/2}$ interpretation is still employed. However, the explanation of $\sqrt{Sc^{-1}(\epsilon t_m)}$ must be expanded. From dimensional considerations alone, this quantity $\sqrt{Sc^{-1}\epsilon t_m}$ is simply the energy content in eddies with characteristic durations t_m acting on the mean scalar concentration difference ΔC when supplied by a constant turbulent energy rate given by ϵ. Hence, t_m may now be impacted by eddies operating on time scales much larger than τ_K. Because the canonical form of k_L does not change under those conditions (i.e., $\propto \sqrt{Sc^{-1}(\epsilon t_m)}$), the factor 2/15 is retained and proportionality constants are determined relative to this original form so as to facilitate an interpolation scheme between all the aforementioned formulations listed in the abstract (via t_m and ϵ).

2.6. Recovering $k_L = \beta Sc^{-1/2} u_*$ (Abstract, iii)

The consistency between equation (16) and the analysis in Csanady (1990) is now considered. The work by Csanady (1990) suggest that for moderate wind speeds, the intense momentum flux exchange is caused by viscous surface stress variations associated with rollers (i.e., circulation zones) on breaking wavelets. The vortical motion is assumed inviscid and spawned from a viscous boundary layer (meaning that its initial surface vorticity scales with u_*/ν and is not altered appreciably in time) on the upwind side of the wavelet. The circulation time around the roller then scales with $\nu/(u_*^2)$. It follows that $t_m = C_m \nu/u_*^2$ instead of τ_k, where C_m is a similarity constant. A naive argument would suggest that

$$k_L = |w_{TO}| = \sqrt{\frac{2}{15}} Sc^{-1/2} \left(\epsilon C_m \frac{\nu}{u_*^2}\right)^{1/2}. \tag{24}$$

The evaluation of ϵ must now be conducted at some distance from a flat interface to reflect the position of wavelets. When setting $\epsilon = u_*^3/(\delta_V)$ (Brutsaert, 1965) and $\delta_V \propto \nu/u_*$ (Lorke & Peeters, 2006; i.e., the expected thickness of the viscous layer for momentum not scalars is $\delta_V \approx 10\nu/u_*$),

$$k_L = |w_{TO}| = \sqrt{\frac{2}{15}} Sc^{-1/2} \left(\frac{u_*^3}{10\nu u_*^{-1}} C_m \frac{\nu}{u_*^2} \right)^{1/2}. \tag{25}$$

That is,

$$k_L = |w_{TO}| = \sqrt{\frac{2}{15}\frac{C_m}{10}} Sc^{-1/2} u_*. \tag{26}$$

Field experiments reporting ϵ profiles below a nonflat water surface suggest some independence of z as the water surface is approached (Wang et al., 2015). Based on the model of Soloviev and Schlüssel (1994), we estimated a $C_m = 0.4$ resulting in a $\beta = 0.073$. This β value is smaller than the one estimated by LP06 ($\beta = 1/9 = 0.11$) from the law-of-the wall over a smooth surface but is in better agreement with the empirical fit to many data sets reported by Jähne and Haußecker (1998; $\beta = 1/16 = 0.065$) and others (Munnich & Flothmann, 1975). In fact,

$$k_L = \frac{1}{16} Sc^{-1/2} u_* \tag{27}$$

was used to estimate the k_L component in the absence of wave-breaking in many field studies focused on the effects of wave breaking on k_L (Shuiqing & Dongliang, 2016). The arguments leading to equation (26) are indeed naive for two reasons: (1) the $r = 2(D_m t_m)^{1/2} = 2(\nu Sc^{-1} t_m)^{1/2}$ are based on scalar transport into a fluid parcel at a flat interface being entirely driven by molecular diffusion with viscosity restricting the diffusion time scale (i.e., momentum transporting eddies are commensurate to η), and (2) the evaluation of ϵ at δ_V (instead of distance r from the interface) is within the viscous boundary layer and is assumed to represent the overall bulk dissipation rate in this entire region (i.e., variation of ϵ with z from the interface are not too significant for quantities that vary as $\epsilon^{1/4}$ such as k_L). Defining a Reynolds number $Re_V = u_* \delta_V/\nu$, then $\eta/\delta_V = Re_V^{-3/4}$. For $\delta_V = 10\nu/u_*$, $\eta/\delta_V \approx (10)^{-3/4} \approx 0.2$ or $\delta_V \approx 5\eta$, consistent with the viscous boundary layer thickness. Moreover, the structure function $r \sim Sc^{-1/2}\delta_V \sim 5Sc^{-1/2}\eta$ remains well below the crossover from inertial to viscous scales for $Sc >> 1$ (i.e., the assumed structure function shape is correct).

It is instructive to compare this formulation with a case where $t_m = C_w u_*/g$ (Csanady, 2001) and $\epsilon = u_*^3/(\kappa z_o)$ (Brutsaert, 1965), with $\kappa = 0.4$ being the von Kármán constant and z_o is the momentum roughness length. In the absence of wave breaking, the momentum roughness length may be estimated by $z_o = a_w u_*^2 g^{-1}$ (Charnock, 1955), which can be used in the determination of the waterside ϵ to yield

$$k_L = |w_{TO}| = \sqrt{\frac{2}{15}} Sc^{-1/2} \left(\frac{u_*^3}{\kappa a_w u_*^2 g^{-1}} C_w \frac{u_*}{g} \right)^{1/2}. \tag{28}$$

A number of reviews have already pointed out that Charnock's equation does not hold for calm conditions or extreme high winds with wave breaking (Wüest & Lorke, 2003). Hence, within the confines of Charnock's equation, k_L reduces to

$$k_L = |w_{TO}| = \sqrt{\frac{2}{15}\frac{C_w}{\kappa a_w}} Sc^{-1/2} u_*. \tag{29}$$

This result is analogous to equation (26). The value of β is further explored. With $C_w \approx 0.18 \times C_m$ (Soloviev & Schlüssel, 1994) and a waterside $a_w = 0.011 \times (\rho/\rho_a)$ yields a $\beta = 0.03$, which is a factor 2 smaller than $\beta = 0.073$ derived from arguments by Csanady (1990). Here the air-side Charnock constant (=0.011) is converted to its waterside counterpart assuming continuity of the dynamic surface stress ($\rho_a u_*^2|_a = \rho u_*^2$) where ρ_a and $u_*|_a$ are the air-side density and friction velocity. This continuity is considered next in the presence of waves and wave breaking at large wind speeds. However, the interpretation of $k_L \propto \sqrt{Sc^{-1}(\epsilon t_m)}$ must now be viewed strictly as an outcome of dimensional considerations as (1) t_m deviates appreciably from τ_K and (2) the uncertainty in ϵ and u_* determination are large. Nonetheless, this consideration does permit a unified model for k_L that spans all the expressions listed in the abstract. This is the main reason this line of inquiry is being pursuit (while mindful of all the model limitations and extrapolations at this stage).

2.7. Recovering $k_L = \gamma Sc^{-1/2}(g\nu/u_*)^{1/2}$ (Abstract, iv)

When surface long waves formed by large wind speeds break down, the surface stress τ_o produced by the wind must be reduced to accommodate the energy carried by waves and the energy used to produce waterside turbulence as related to the tangential stress τ_t. This partitioning is achieved by using the Keulegan number $Ke = u_*^3/(g\nu)$ so that

$$\tau_t = \frac{\tau_o}{1 + Ke/Ke_c}, \tag{30}$$

where $Ke_c \approx 0.18$ is a critical Keulegan number that determines the crossover from wavelet- to long-wave breaking (Csanady, 2001; Soloviev & Schlüssel, 1994; Soloviev, 2007). Assuming that the waterside $\epsilon = (\tau_t/\rho)u_*/(\kappa z_o)$ and repeating the above analysis with $t_m = C_w u_*/g$ yields

$$k_L = |w_{TO}| = \sqrt{\frac{2}{15}\frac{C_w}{\kappa a_w}}Sc^{-1/2}\frac{u_*}{\sqrt{1 + Ke/Ke_c}}. \tag{31}$$

When $Ke << Ke_c$, then equation (29) is recovered. However, for $Ke >> Ke_c$ (long-wave breaking), then equation (31) becomes

$$k_L = |w_{TO}| = \sqrt{\frac{2}{15}\frac{Ke_c C_w}{\kappa a_w}}Sc^{-1/2}\sqrt{\frac{g\nu}{u_*}}, \tag{32}$$

which is identical to equation (6) with $\gamma = 0.03Ke_c^{1/2}$. The connection between Ke and the critical number for wind-wave breaking is now highlighted using arguments similar to Soloviev (2007). As discussed by Zhao and Toba (2001), a dimensionless number R_B empirically characterizing the onset of wind-wave breaking is

$$R_B = \frac{u_*^2|_a}{\nu_a \omega_p} = 1000, \tag{33}$$

where ν_a is the air viscosity, $\omega_p = g/(A_w u_*|_a)$ is the peak angular frequency of wind waves, and A_w is the wave age (defined as wave speed normalized by $u_*|_a$). This threshold R_B and ω_p have received significant theoretical attention and experimental support (Melville & Rapp, 1985; Shuiqing & Dongliang, 2016; Zhao et al., 2003). Specifying a critical $Ke_c = (u_*|_c)^3/(g\nu)$ is a kin to setting a threshold R_B for a given A_w, where $u_*|_c$ is the critical waterside friction velocity responsible for the formation of long surface waves. Starting with the definition of R_B, the following expression can be derived:

$$R_B = \left(\frac{\rho_w}{\rho_a}\right)^{3/2}\left(\frac{\nu}{\nu_a}\right)A_w Ke, \tag{34}$$

Interestingly, for a threshold $R_B = 1000$ and $Ke_c = 0.18$ independently derived by Soloviev and Schlüssel (1994), an $A_w = 3.25$ may be inferred. This wave age corresponds to the early stages of surface long-wave development ($A_w \approx 4$) as discussed elsewhere (Csanady, 2001). As earlier noted, the arguments leading to equation (6) miss the enhanced dissipation rate due to wave breaking, which was not explicitly considered by Soloviev and Schlüssel (1994). However, the point here is that when forcing equation (16) with constraints similar to those used in surface renewal theories for long surface waves, their main k_L predictions (Soloviev & Schlüssel, 1994) can be recovered from the structure function model proposed here.

2.8. A unified model for $Ke/Ke_c < 1$

Combining all the aforementioned estimates of ϵ and t_m, a single model for k_L that accommodates thermal stratification, wavelets and waves can be derived. Thermal stratification (i.e., Ri_f) is introduced by ϵ in equation (17). The Ke is introduced by considering the mechanical production term in equation (17) assuming only the turbulent stress (not the mean velocity gradient) is modified by equation (30). This combination of assumptions can be expressed in a *Csanady-form* as

$$k_L = \sqrt{\frac{2}{15}}\left[\sqrt{\frac{1 - Ri_f}{1 + Ke/Ke_c}\left(\frac{dU}{dz}t_m\right)}\right]Sc^{-1/2}u_*. \tag{35}$$

Here dU/dz is the mean vorticity and t_m is an effective turnover time scale. If the effect of thermal stratification on dU/dz is ignored for simplicity, then $dU/dz = u_*/\delta$ and

$$k_L = \sqrt{\frac{2}{15}}\left[\sqrt{\frac{1-Ri_f}{1+Ke/Ke_c}A_c}\right] Sc^{-1/2}u_*, \tag{36}$$

and where $A_c = u_* t_m/\delta$ is a constant when $Ke/Ke_c < 1$. This condition is analogous to the modified *turbulent interface law* proposed by Csanady (1978). When $Ke/Ke_c < 1$, then $\delta = 10\nu/u_*$ (thickness of the viscous sublayer) and $t_m = C_m\nu/u_*^2$ so that $A_c = u_* t_m/\delta = C_m/10$ (with $C_m = 0.4$). That is, the presence of wavelets do not disturb appreciably δ from its viscous-sublayer estimate.

When $Ke/Ke_c > 1$, as may be expected for very high wind speeds, then long waves form and δ now scales with wave properties such as wave age. In the naive case of a wave height scaling as $\delta = a' u_*^2/g$ and $t_m = C_w u_*/g$, where $C_w = Ke_c C_m = 0.18\times0.4$. Again, $A_c = u_* t_m/\delta$ is a constant that now varies with wave age or the constant a' (i.e., $u_* t_m/\delta = C_w/a'$ is constant). This unified formulation recovers the comprehensive surface renewal model of Soloviev and Schlüssel (1994) with the aforementioned caveats of decline in k_L with increasing u_* for $Ke/Ke_c > 1$. None of the experiments support a decline in k_L for such conditions (Ho et al., 2006; Wanninkhof et al., 2009). For such conditions, bubble transport becomes a significant contributor to k_L and is not considered here. Renewal formulations correcting for the role of bubbles assume that k_L is a linear superposition of a hydrodynamic term (i.e., analogous to predictions from equation (36) and a bubble transport term that is separately modeled as proposed elsewhere(Soloviev & Schlüssel, 1994). The hydrodynamic contributions to k_L by such surface renewal schemes exhibit a decline with increased mean wind speed at very large wind speeds.

3. Model Limitation

The limitations of the approach are now reviewed. The work here only focused on clear water surfaces with no surfactants. Surfactants introduce finite interfacial stresses at the air-water interface that then create a highly dissipative viscous layer (i.e., the air-water interface begins to resemble a solid wall in the limit of high viscous damping). As such, surfactants are expected to retard gas exchange significantly across the air-water interface. Notwithstanding this complication, a number of studies suggest that the effects of surfactants can be accommodated by varying the exponent n in $k_L \propto Sc^{-n}$ as discussed elsewhere (McKenna & McGillis, 2004). Notably, it was shown that

$$n \approx \frac{2}{3} - \frac{1}{6}\exp\left(-2\Lambda\right), \tag{37}$$

where Λ is the ratio of the Marangoni stress (related to surfactant concentration) to a virtual viscous stress due to a rigid wall. That is, Λ provides a dimensionless number that assess to what degree the surface resembles an immobile boundary. For $\Lambda = 0$ (clean surface), $n = 1/2$ (as predicted by surface renewal and structure function approaches). However, as $\Lambda \to 1$ (Marangoni stress is comparable to the viscous stress in wall-bounded flows with $\partial w/\partial z \to 0$), $n \to 2/3$, which is the canonical value for wall-bounded flow; Csanady, 2001; Deacon, 1977. Another limitation is that the formulations here did not consider bubble contributions to k_L, which are expected to be significant for large wind speed and long-wave conditions.

The approach is entirely anchored to the von Kármán-Howarth equation describing $D_{ww}(r)$. This equation and approximate solutions to it are based on locally homogeneous and isotropic turbulence. This assumption is clearly violated near the air-water interface at large scales ($r/\eta >> 1$), though it may be reasonable for small eddy sizes ($r \approx 2l_B$). Another limitation is the absence of a rigorous link between molecular diffusion at the water surface and eddy transport just below the water surface. The structure function approach here packs them into l_B or their effect on t_m. This scaling appears reasonable when $Sc >> 1$, as discussed elsewhere (Lorke & Peeters, 2006). However, finite $D_{ww}(r)/r^2$ as $r \sim l_B$ implies that $\partial w'/\partial z$ must be finite near the interface. A consequence of a finite $\partial w'/\partial z$ is that the approach must lead to $k_L \sim Sc^{-1/2}$ and cannot predict other scaling exponents (e.g., $k_L \sim Sc^{-2/3}$). At the most generic level, the structure function approach provides a link between k_L, ϵ, and a diffusion time t_m (i.e., $k_L \propto (\epsilon t_m)^{1/2}$). To recover prior formulations, choices for t_m and models for ϵ are needed and those choices also introduce their own limitations. The simplest model for ϵ may be derived from an idealized stationary and planar-homogeneous TKE budget with no mean vertical velocity and where production and dissipation rates of TKE are in balance. This assumption, while common to many air-sea gas exchange studies, misses important nonlocal TKE transport mechanisms associated with

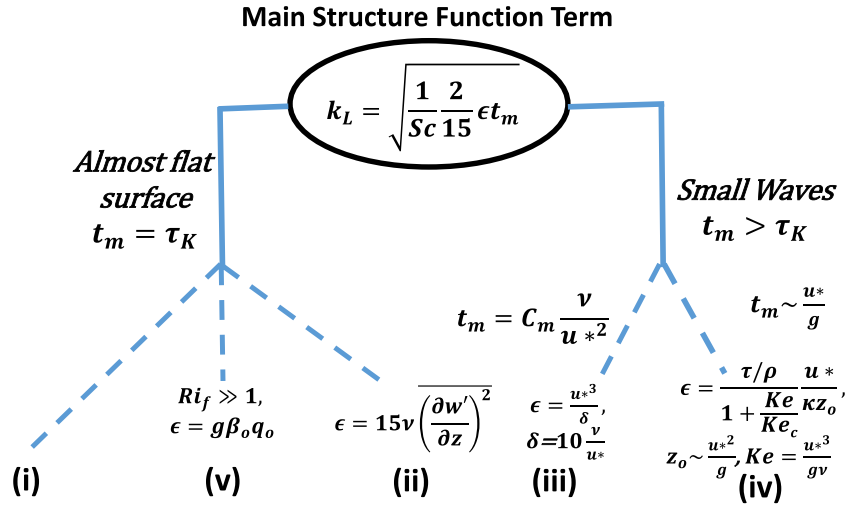

Figure 2. Summary of assumptions about t_m and ϵ used to arrive at equations (i)–(iv) presented in the abstract. The main term is derived from approximations to the von Kármán-Howarth equation that accounts for a balance between energy transfer across scales, vortex stretching and viscous diffusion. Expressions for $t_m > \tau_K$ must be viewed as ad hoc but plausible. Dimensional considerations alone would suggest that $k_L \propto \sqrt{\epsilon t_m}$, where t_m may be interpreted as turnover time.

turbulence and mean advective terms. These mechanisms result in ϵ being underestimated when inferred from production and buoyancy terms alone. The fact that $k_L \sim \epsilon^{1/4}$ also means that a factor of 2 adjustments to inferred ϵ translates to only a factor of 1.18 adjustment to k_L. The choices made about t_m have been discussed at length for almost flat surfaces and small waves. For almost flat surfaces, the choice $t_m = \tau_K$ (i.e., the Kolmogorov time scale) recovers prior results with the added foresight for the associated similarity constants. For the energetic-eddy hypothesis, the $t_m = Re_t^{1/2}\tau_K$ also recovers the α dependency on Reynolds numbers for $Re_t < 500$ supported by DNS and experiments. For wavy surfaces, the results derived here must be viewed with caution given that t_m may be much larger than τ_K and other constraints on eddy sizes beyond $r = 2(D_m t_m)^{1/2}$ must be factored in. When extrapolating to such wavy surfaces, the quantity $(\epsilon t_m)^{1/2}$ was broadly interpreted as energy content in eddies of turnover duration t_m supplied by an energy rate ϵ. The consistency between this outcome and prior formulations derived from detailed surface renewal schemes or other dynamical considerations (Csanady, 1990) certainly warrants further inquiry, a topic best left for future work.

4. Conclusion

The work here shows how multiple k_L expressions can be derived from a single expression (i.e., equation (16). This equation is derived using the shape of the vertical velocity structure function for locally homogeneous and isotropic turbulence near the air-water interface. It shows that all five k_L expressions listed in the abstract are recovered by choosing an appropriate diffusion time scale and estimates of the TKE dissipation rate as summarized in Figure 2. In particular, when the diffusion time scale is set to the Kolmogorov time scale, $k_L = \sqrt{2/15}Sc^{-1/2}(\nu\epsilon)^{1/4}$. In the presence of wavelets, the diffusion time $t_m = C_m\nu/u_*^2$ and $k_L = \sqrt{2/15C_m/10}Sc^{-1/2}u_*$, where $C_m = 0.4$ was determined from independent experiments. In the presence of long waves and when t_m scales with u_*/g as expected from Charnock's equation, $k_L \propto Sc^{-1/2}\sqrt{g\nu/u_*}$. The latter condition further requires a Keulegan number exceeding a critical value of 0.18 to ensure the generation of long surface waves. It is noted that while these results agree with prior surface renewal theories (Soloviev, 2007; Soloviev & Schlüssel, 1994), they emerge from the assumed shape of the vertical velocity structure function. Last, the effect of buoyancy is explicitly included and the limits associated with free convection recovered.

Appendix A: Linkage Between Eddy Size and the Batchelor Scale

The rational for selecting eddy size $r \approx 2l_B$ is presented, where $l_B = \sqrt{D_m\tau_K}$ is the Batchelor scale, τ_K is the Kolmogorov microscale representing the turnover time of this eddy, and D_m is the molecular diffusion

coefficient. For this effective eddy of size r to allow efficient mass exchange between the air-water interface and the bulk region, its size must span the thickness of the diffusive layer δ_D (i.e., $r \approx \delta_D$). Dimensional analysis presented in section 2 already suggested that $\delta_D \propto \sqrt{D_m \tau_K}$ or $\delta_D \approx r \propto l_B$. The premise here is that within the diffusive layer, mass transport over a turnover time period τ_K is primarily dominated by molecular diffusion. Dimensional analysis alone cannot provide the value of the proportionality constant. To do so requires an estimate of δ_D by other means such as the diffusion equation applied within the diffusive layer. The diffusive layer is bounded by the air-water interface characterized by concentration C_s and a bulk region characterized by concentration C_b. Mass transport within the diffusive layer is governed by

$$\frac{\partial C}{\partial t} = D_m \frac{\partial^2 C}{\partial z^2}, \tag{A1}$$

where t is time and z is depth from the air-water interface. This equation is subject to two boundary conditions:

$$C(t, 0) = C_s; C(t, z \to \infty) = C_b. \tag{A2}$$

Using the Boltzmann transform

$$\xi = \frac{z}{2\sqrt{D_m t}}, \tag{A3}$$

reduces the diffusion equation into a second-order ordinary differential equation given by

$$-2\xi \frac{dC}{d\xi} = D_m \frac{d^2 C}{d\xi^2}. \tag{A4}$$

Imposing the two boundary conditions yields

$$\frac{C(\xi) - C_s}{C_b - C_s} = \text{erf}(\xi), \tag{A5}$$

where the erf(.) is the error function. The diffusive distance z that would have occurred over $t = \tau_K$ can be determined from

$$\frac{C(\xi) - C_s}{C_b - C_s} = \text{erf}\left(\frac{z}{2l_B}\right). \tag{A6}$$

If delineation of boundary layer thickness (i.e., $z = \delta_V$) is based on 90% attainment of relative concentration change, then

$$\text{erf}\left(\frac{\delta_V}{2l_B}\right) = 0.9, \tag{A7}$$

resulting in $r = \delta_V \approx 1.16(2l_B)$, which, for simplicity, was selected as $\delta_V = r = (2l_B)$ in the main text. It is to be noted that a 95% and a 99% attainment of bulk concentrations would have yielded $\delta_V \approx 1.36(2l_B)$ and $\delta_V \approx 1.82(2l_B)$. With these stricter definitions of boundary layer thickness, the similarity coefficient α in equation (2) increases to $\alpha = \sqrt{1.38 \times (2/15)} = 0.43$ and $\alpha = \sqrt{1.82 \times (2/15)} = 0.49$, respectively.

Acknowledgments
G.K. acknowledges support from the National Science Foundation (NSF-AGS-1644382, NSF-EAR-1344703, and NSF-DGE-1068871), the U.S. Department of Energy (DOE) through the office of Biological and Environmental Research (BER) Terrestrial Ecosystem Science (TES) Program (DE-SC0006967 and DE-SC0011461), and the MICMoR fellows program at KIT/IMF-IFU (in Garmisch-Partenkirchen, Germany). T.V., I.M., and T.G. acknowledge support from the Academy of Finland Center of Excellence (projects No. 272041 and 118780), the Academy Professor projects (No. 1284701 and 1282842), ICOS-Finland (project No. 281255), CarLAC (project no. 281196) sponsored by the Academy of Finland, the AtMath project funded by University of Helsinki (Finland), and the EU-project GHG-LAKE (project no. 612642). The work is theoretical in nature and no data are presented.

References

Asher, W. E., Jessup, A. T., & Atmane, M. A. (2004). Oceanic application of the active controlled flux technique for measuring air-sea transfer velocities of heat and gases. *Journal of Geophysical Research*, *109*. https://doi.org/10.1029/2003JC001862

Banerjee, S., Lakehal, D., & Fulgosi, M. (2004). Surface divergence models for scalar exchange between turbulent streams. *International Journal of Multiphase Flow*, *30*(7), 963–977.

Bastviken, D., Tranvik, L. J., Downing, J. A., Crill, P. M., & Enrich-Prast, A. (2011). Freshwater methane emissions offset the continental carbon sink. *Science*, *331*(6013), 50–50.

Batchelor, G. (1959). Small-scale variation of convected quantities like temperature in turbulent fluid Part 1. General discussion and the case of small conductivity. *Journal of Fluid Mechanics*, *5*(01), 113–133.

Bell, T., De Bruyn, W., Miller, S., Ward, B., Christensen, K., & Saltzman, E. (2013). Air–sea dimethylsulfide (dms) gas transfer in the North Atlantic: Evidence for limited interfacial gas exchange at high wind speed. *Atmospheric Chemistry and Physics*, *13*(21), 11,073–11,087.

Bell, T. G., Landwehr, S., Miller, S. D., Bruyn, W. J. d., Callaghan, A. H., Scanlon, B., et al. (2017). Estimation of bubble-mediated air–sea gas exchange from concurrent DMS and CO_2 transfer velocities at intermediate–high wind speeds. *Atmospheric Chemistry and Physics*, *17*(14), 9019–9033.

Berg, P., & Pace, M. L. (2017). Continuous measurement of air–water gas exchange by underwater eddy covariance. *Biogeosciences*, *14*(23), 5595.

Bigdeli, A., Hara, T., Loose, B., & Nguyen, A. (2018). Wave attenuation and gas exchange velocity in marginal sea ice zone. *Journal of Geophysical Research: Oceans*, *123*, 2293–2304. https://doi.org/10.1002/2017JC013380
Bolin, B. (1960). On the exchange of carbon dioxide between the atmosphere and the sea. *Tellus*, *12*(3), 274–281. https://doi.org/10.1111/j.2153-3490.1960.tb01311.x
Brumley, B. H., & Jirka, G. H. (1987). Near-surface turbulence in a grid-stirred tank. *Journal of Fluid Mechanics*, *183*, 235–263.
Brutsaert, W. (1965). A model for evaporation as a molecular diffusion process into a turbulent atmosphere. *Journal of Geophysical Research*, *70*(20), 5017–5024.
Brutsaert, W. (1975). A theory for local evaporation (or heat transfer) from rough and smooth surfaces at ground level. *Water resources research*, *11*, 543–550.
Butman, D., & Raymond, P. A. (2011). Significant efflux of carbon dioxide from streams and rivers in the United States. *Nature Geoscience*, *4*(12), 839.
Charnock, H. (1955). Wind stress on a water surface. *Quarterly Journal of the Royal Meteorological Society*, *81*(350), 639–640.
Chu, C. R., & Jirka, G. H. (2003). Wind and stream flow induced reaeration. *Journal of Environmental Engineering*, *129*(12), 1129–1136.
Cole, J. J., Bade, D. L., Bastviken, D., Pace, M. L., & Van de Bogert, M. (2010). Multiple approaches to estimating air-water gas exchange in small lakes. *Limnology and Oceanography: Methods*, *8*(6), 285–293.
Cornish, V. (1909). Wind-waves in water, sand, snow, and cloud. *Quarterly Journal of the Royal Meteorological Society*, *35*(151), 149–160.
Csanady, G. T. (1978). Turbulent interface layers. *Journal of Geophysical Research*, *83*(C5), 2329–2342.
Csanady, G. (1990). The role of breaking wavelets in air-sea gas transfer. *Journal of Geophysical Research*, *95*(C1), 749–759.
Csanady, G. T. (2001). *Air-sea interaction: Laws and mechanisms*. New York: Cambridge University Press.
Davidson, P. (2015). *Turbulence: An introduction for scientists and engineers*. Oxford, UK: Oxford University Press.
Deacon, E. (1977). Gas transfer to and across an air-water interface. *Tellus*, *29*(4), 363–374.
Dobler, W., Haugen, N. E. L., Yousef, T. A., & Brandenburg, A. (2003). Bottleneck effect in three-dimensional turbulence simulations. *Physical Review E*, *68*, 026304. https://doi.org/10.1103/PhysRevE.68.026304
Donzis, D., & Sreenivasan, K. (2010). The bottleneck effect and the Kolmogorov constant in isotropic turbulence. *Journal of Fluid Mechanics*, *657*, 171–188.
Esters, L., Landwehr, S., Sutherland, G., Bell, T., Christensen, K., Saltzman, E., et al. (2017). Parameterizing air-sea gas transfer velocity with dissipation, *122*, 3041–3056. https://doi.org/10.1002/2016JC012088
Fortescue, G., & Pearson, J. (1967). On gas absorption into a turbulent liquid. *Chemical Engineering Science*, *22*(9), 1163–1176.
Foster, T. (1971). Intermittent convection. *Geophysical and Astrophysical Fluid Dynamics*, *2*(1), 201–217.
Fredriksson, S. T., Arneborg, L., Nilsson, H., Zhang, Q., & Handler, R. A. (2016). An evaluation of gas transfer velocity parametrization during natural convection using DNS. *Journal of Geophysical Research: Oceans*, *121*, 1400–1423. https://doi.org/10.1002/2015JC011112
Frisch, U., Kurien, S., Pandit, R., Pauls, W., Ray, S. S., Wirth, A., & Zhu, J.-Z. (2008). Hyperviscosity, Galerkin truncation, and bottlenecks in turbulence. *Physical Review Letters*, *101*(14), 144501.
Frisch, U., Ray, S. S., Sahoo, G., Banerjee, D., & Pandit, R. (2013). Real-space manifestations of bottlenecks in turbulence spectra. *Physical Review Letters*, *110*(6), 064501.
Frost, T., & Upstill-Goddard, R. (1999). Air-sea gas exchange into the millenium: Progress and uncertainties. *Oceanography and Marine Biology: An Annual Review*, *377*, 1–45.
Galperin, B., Sukoriansky, S., & Anderson, P. S. (2007). On the critical Richardson number in stably stratified turbulence. *Atmospheric Science Letters*, *8*(3), 65–69.
Garbe, C. S., Rutgersson, A., Boutin, J., De Leeuw, G., Delille, B., Fairall, C. W., et al. (2014). Transfer across the air-sea interface. In *Ocean-atmosphere interactions of gases and particles* (pp. 55–112). Berlin: Springer.
Garbe, C. S., Schimpf, U., & Jähne, B. (2004). A surface renewal model to analyze infrared image sequences of the ocean surface for the study of air-sea heat and gas exchange. *Journal of Geophysical Research*, *109*, C08S15. https://doi.org/10.1029/2003JC001802
Genereux, D. P., & Hemond, H. F. (1992). Determination of gas exchange rate constants for a small stream on Walker Branch Watershed, Tennessee. *Water Resources Research*, *28*(9), 2365–2374.
Grachev, A. A., Andreas, E. L., Fairall, C. W., Guest, P. S., & Persson, P. O. G. (2013). The critical Richardson number and limits of applicability of local similarity theory in the stable boundary layer. *Boundary-Layer Meteorology*, *147*, 1–32.
Haghighi, E., & Or, D. (2013). Evaporation from porous surfaces into turbulent airflows: Coupling eddy characteristics with pore scale vapor diffusion. *Water Resources Research*, *49*(12), 8432–8442. https://doi.org/10.1002/2012WR013324
Hasse, L. (1980). Gas exchange across the air–sea interface. *Tellus*, *32*(5), 470–481.
Heiskanen, J. J., Mammarella, I., Haapanala, S., Pumpanen, J., Vesala, T., MacIntyre, S., & Ojala, A. (2014). Effects of cooling and internal wave motions on gas transfer coefficients in a boreal lake. *Tellus B*, *66*, 22827. https://doi.org/10.3402/tellusb.v66.22827
Herlina, H., & Wissink, J. (2014). Direct numerical simulation of turbulent scalar transport across a flat surface. *Journal of Fluid Mechanics*, *744*, 217–249.
Herring, J. R., Schertzer, D., Lesieur, M., Newman, G. R., Chollet, J. P., & Larcheveque, M. (1982). A comparative assessment of spectral closures as applied to passive scalar diffusion. *Journal of Fluid Mechanics*, *124*, 411–437. https://doi.org/10.1017/S0022112082002560
Hill, R. (1978). Models of the scalar spectrum for turbulent advection. *Journal of Fluid Mechanics*, *88*, 541–562.
Ho, D. T., Law, C. S., Smith, M. J., Schlosser, P., Harvey, M., & Hill, P. (2006). Measurements of air-sea gas exchange at high wind speeds in the Southern Ocean: Implications for global parameterizations. *Geophysical Research Letters*, *33*. https://doi.org/10.1029/2006GL026817
Hondzo, M. (1998). Dissolved oxygen transfer at the sediment-water interface in a turbulent flow. *Water Resources Research*, *34*(12), 3525–3533.
Huebert, B. J., Blomquist, B. W., Hare, J., Fairall, C., Johnson, J. E., & Bates, T. S. (2004). Measurement of the sea-air DMS flux and transfer velocity using eddy correlation. *Geophysical Research Letters*, *31*(23). https://doi.org/10.1029/2004GL021567
Huotari, J., Ojala, A., Peltomaa, E., Nordbo, A., Launiainen, S., Pumpanen, J., et al. (2011). Long-term direct CO_2 flux measurements over a boreal lake: Five years of eddy covariance data. *Geophysical Research Letters*, *38*, L18401. https://doi.org/10.1029/2011GL048753
Jähne, B., & Haußecker, H. (1998). Air-water gas exchange. *Annual Review of Fluid Mechanics*, *30*(1), 443–468.
Katul, G. G., Banerjee, T., Cava, D., Germano, M., & Porporato, A. (2016). Generalized logarithmic scaling for high-order moments of the longitudinal velocity component explained by the random sweeping decorrelation hypothesis. *Physics of Fluids*, *28*(9), 095104.
Katul, G., & Liu, H. (2017a). Multiple mechanisms generate a universal scaling with dissipation for the air-water gas transfer velocity. *Geophysical Research Letters*, *44*, 1892–1898. https://doi.org/10.1002/2016GL072256
Katul, G., & Liu, H. (2017b). A Kolmogorov-Brutsaert structure function model for evaporation into a turbulent atmosphere. *Water Resources Research*, *53*, 3635–3644. https://doi.org/10.1002/2016WR020006

Katul, G., Manes, C., Porporato, A., Bou-Zeid, E., & Chamecki, M. (2015). Bottlenecks in turbulent kinetic energy spectra predicted from structure function inflections using the von Kármán-Howarth equation. *Physical Review E*, *92*(033009). https://doi.org/10.1103/PhysRevE.92.033009

Katul, G. G., Porporato, A., Shah, S., & Bou-Zeid, E. (2014). Two phenomenological constants explain similarity laws in stably stratified turbulence. *Physical Review E*, *89*(2), 023007.

Kermani, A., & Shen, L. (2009). Surface age of surface renewal in turbulent interfacial transport. *Geophysical Research Letters*, *36*, L10605. https://doi.org/10.1029/2008GL037050

Kitaigorodskii, S. (1984). On the fluid dynamical theory of turbulent gas transfer across an air-sea interface in the presence of breaking wind-waves. *Journal of Physical Oceanography*, *14*(5), 960–972.

Kolmogorov, A. N. (1941). The local structure of turbulence in incompressible viscous fluid for very large Reynolds numbers. In *Dokl. Akad. Nauk SSSR* (Vol. 30, pp. 301–305). Moscow.

Komori, S., Nagaosa, R., & Murakami, Y. (1990). Mass transfer into a turbulent liquid across the zero-shear gas-liquid interface. *AIChE journal*, *36*(6), 957–960.

Komori, S., Nagaosa, R., & Murakami, Y. (1993). Turbulence structure and mass transfer across a sheared air–water interface in wind-driven turbulence. *Journal of Fluid Mechanics*, *249*, 161–183.

Koopmans, D. J., & Berg, P. (2015). Stream oxygen flux and metabolism determined with the open water and aquatic eddy covariance techniques. *Limnology and Oceanography*, *60*(4), 1344–1355.

Lamont, J. C., & Scott, D. (1970). An eddy cell model of mass transfer into the surface of a turbulent liquid. *AIChE Journal*, *16*(4), 513–519.

Ledwell, J. J. (1984). The variation of the gas transfer coefficient with molecular diffusity. In *Gas transfer at water surfaces* (pp. 293–302.). Dordrecht, Netherlands: Springer.

Lewis, W., & Whitman, W. (1924). Principles of gas absorption. *Industrial & Engineering Chemistry*, *16*(12), 1215–1220.

Li, D., Katul, G. G., & Zilitinkevich, S. S. (2015). Revisiting the turbulent Prandtl number in an idealize atmospheric surface layer. *Journal of the Atmospheric Sciences*, *72*(6), 2394–2410.

Li, D., Katul, G. G., & Zilitinkevich, S. S. (2016). Closure schemes for stably stratified atmospheric flows without turbulence cutoff. *Journal of the Atmospheric Sciences*, *73*(12), 4817–4832.

Liss, P. S., Marandino, C. A., Dahl, E. E., Helmig, D., Hintsa, E. J., Hughes, C., et al. (2014). Short-lived trace gases in the surface ocean and the atmosphere. In *Ocean-Atmosphere Interactions of Gases and Particles* (pp. 1–54). Berlin, Germany: Springer.

Liu, H., Zhang, Q., Katul, G. G., Cole, J. J., Chapin, F. S. III, & MacIntyre, S. (2016). Large CO_2 effluxes at night and during synoptic weather events significantly contribute to CO_2 emissions from a reservoir. *Environmental Research Letters*, *11*(6), 064001.

Lorke, A., & Peeters, F. (2006). Toward a unified scaling relation for interfacial fluxes. *Journal of Physical Oceanography*, *36*(5), 955–961.

MacIntyre, S., Jonsson, A., Jansson, M., Aberg, J., Turney, D. E., & Miller, S. D. (2010). Buoyancy flux, turbulence, and the gas transfer coefficient in a stratified lake. *Geophysical Research Letters*, *37*, L24604. https://doi.org/10.1029/2010GL044164

Mammarella, I., Nordbo, A., Rannik, Ü., Haapanala, S., Levula, J., Laakso, H., et al. (2015). Carbon dioxide and energy fluxes over a small boreal lake in Southern Finland. *Journal of Geophysical Research: Biogeosciences*, *120*, 1296–1314. https://doi.org/10.1002/2014JG002873

Marx, A., Dusek, J., Jankovec, J., Sanda, M., Vogel, T., Geldern, R., et al. (2017). A review of CO_2 and associated carbon dynamics in headwater streams: A global perspective. *Reviews of Geophysics*, *55*, 560–585.

McColl, K. A., Katul, G. G., Gentine, P., & Entekhabi, D. (2016). Mean-velocity profile of smooth channel flow explained by a cospectral budget model with wall-blockage. *Physics of Fluids*, *28*(3), 035107.

McCready, M., Vassiliadou, E., & Hanratty, T. (1986). Computer simulation of turbulent mass transfer at a mobile interface. *AIChE Journal*, *32*(7), 1108–1115.

McKenna, S., & McGillis, W. (2004). The role of free-surface turbulence and surfactants in air–water gas transfer. *International Journal of Heat and Mass Transfer*, *47*(3), 539–553.

Melville, W., & Rapp, R. J. (1985). Momentum flux in breaking waves. *Nature*, *317*(6037), 514–516.

Memery, L., & Merlivat, L. (1985). Modelling of gas flux through bubbles at the air-water interface. *Tellus B*, *37*(4-5), 272–285.

Meyers, J., & Meneveau, C. (2008). A functional form for the energy spectrum parameterizing bottleneck and intermittency effects. *Physics of Fluids (1994-present)*, *20*(6), 065109. https://doi.org/10.1063/1.2936312

Monin, A., & Yaglom, A. (1975). *Statistical fluid mechanics, volume II: Mechanics of turbulence* (Vol. 2). Boston: MIT Press.

Munnich, K., & Flothmann, D. (1975). Gas exchange in relation to other air/sea interaction phenomena. In *SCOR Workshop on Air/sea Interaction Phenomena*, *8* (pp. 12). Miami, FL. Zenodo https://doi.org/10.5281/zenodo.13345

Ouellette, N. T., Xu, H., Bourgoin, M., & Bodenschatz, E. (2006). Small-scale anisotropy in Lagrangian turbulence. *New Journal of Physics*, *8*(6), 102–112. https://doi.org/10.1088/1367-2630/8/6/102

Pope, S. B. (2000). *Turbulent flows* (pp. 771). Cambridge, UK: Cambridge University Press.

Prata, A. A., Santos, J. M., Timchenko, V., & Stuetz, R. M. (2017). A critical review on liquid-gas mass transfer models for estimating gaseous emissions from passive liquid surfaces in wastewater treatment plants. *Water Research*, *130*, 388–406. https://doi.org/doi.org/10.1016/j.watres.2017.12.001

Rantakari, M., Heiskanen, J., Mammarella, I., Tulonen, T., Linnaluoma, J., Kankaala, P., & Ojala, A. (2015). Different apparent gas exchange coefficients for CO_2 and CH_4: Comparing a brown-water and a clear-water lake in the boreal zone during the whole growing season. *Environmental Science & Technology*, *49*(19), 11,388–11,394.

Rao, K. N., Narasimha, R., & Narayanan, M. B. (1971). The bursting phenomenon in a turbulent boundary layer. *Journal of Fluid Mechanics*, *48*(02), 339–352.

Raymond, P. A., & Cole, J. J. (2001). Gas exchange in rivers and estuaries: Choosing a gas transfer velocity. *Estuaries and Coasts*, *24*(2), 312–317.

Raymond, P. A., Hartmann, J., Lauerwald, R., Sobek, S., McDonald, C., Hoover, M., et al. (2013). Global carbon dioxide emissions from inland waters. *Nature*, *503*(7476), 355–359.

Rossby, C.-G., & Montgomery, R. B. (1935). *The layer of frictional influence in wind and ocean currents* (pp. 1–100). Cambridge: Massachusetts Institute of Technology and Woods Hole Oceanographic Institution.

Saddoughi, S., & Veeravalli, S. (1994). Local isotropy in turbulent boundary layers at high Reynolds number. *Journal of Fluid Mechanics*, *268*, 333–372.

Shahraeeni, E., Lehmann, P., & Or, D. (2012). Coupling of evaporative fluxes from drying porous surfaces with air boundary layer: Characteristics of evaporation from discrete pores. *Water Resources Research*, *48*, W09525. https://doi.org/doi.org/10.1029/2012WR011857

Shuiqing, L., & Dongliang, Z. (2016). Gas transfer velocity in the presence of wave breaking. *Tellus B*, *68*, 27034. https://doi.org/10.3402/tellusb.v68.27034

Soloviev, A. V. (2007). Coupled renewal model of ocean viscous sublayer, thermal skin effect and interfacial gas transfer velocity. *Journal of Marine Systems*, *66*(1), 19–27.
Soloviev, A. V., & Schlüssel, P. (1994). Parameterization of the cool skin of the ocean and of the air-ocean gas transfer on the basis of modeling surface renewal. *Journal of Physical Oceanography*, *24*(6), 1339–1346.
Takagaki, N., Kurose, R., Kimura, A., & Komori, S. (2016). Effect of Schmidt number on mass transfer across a sheared gas-liquid interface in a wind-driven turbulence. *Scientific Reports*, *6*, 37059. https://doi.org/10.1038/srep37059
Tedford, E. W., MacIntyre, S., Miller, S. D., & Czikowsky, M. J. (2014). Similarity scaling of turbulence in a temperate lake during fall cooling. *Journal of Geophysical Research: Oceans*, *119*, 4689–4713. https://doi.org/10.1002/2014JC010135
Tennekes, H., & Lumley, J. L. (1972). *A first course in turbulence*. Massachusetts: MIT press.
Theofanous, T., Houze, R., & Brumfield, L. (1976). Turbulent mass transfer at free, gas-liquid interfaces, with applications to open-channel, bubble and jet flows. *International Journal of Heat and Mass Transfer*, *19*(6), 613–624.
Tokoro, T., Kayanne, H., Watanabe, A., Nadaoka, K., Tamura, H., Nozaki, K., et al. (2008). High gas-transfer velocity in coastal regions with high energy-dissipation rates. *Journal of Geophysical Research*, *113*, C11006. https://doi.org/10.1029/2007JC004528
Upstill-Goddard, R. C. (2006). Air–sea gas exchange in the coastal zone. *Estuarine Coastal and Shelf Science*, *70*(3), 388–404.
Vachon, D., Prairie, Y. T., & Cole, J. J. (2010). The relationship between near-surface turbulence and gas transfer velocity in freshwater systems and its implications for floating chamber measurements of gas exchange. *Limnology and Oceanography*, *55*(4), 1723. https://doi.org/10.4319/lo.2010.55.4.1723
Vlahos, P., & Monahan, E. C. (2009). A generalized model for the air-sea transfer of dimethyl sulfide at high wind speeds. *Geophysical Research Letters*, *36*, L21605. https://doi.org/10.1029/2009GL040695
von Kármán, T., & Howarth, L. (1938). On the statistical theory of isotropic turbulence. *Proceedings of the Royal Society A*, *164*, 192–216.
Wüest, A., & Lorke, A. (2003). Small-scale hydrodynamics in lakes. *Annual Review of Fluid Mechanics*, *35*(1), 373–412.
Wang, B., Liao, Q., Fillingham, J. H., & Bootsma, H. A. (2015). On the coefficients of small eddy and surface divergence models for the air-water gas transfer velocity. *Journal of Geophysical Research: Oceans*, *120*, 2129–2146. https://doi.org/10.1002/2014JC010253
Wanninkhof, R., Asher, W. E., Ho, D. T., Sweeney, C., & McGillis, W. R. (2009). Advances in quantifying air-sea gas exchange and environmental forcing. *Annual Review of Marine Science*, *1*, 213–244.
Woolf, D. K., & Thorpe, S. (1991). Bubbles and the air-sea exchange of gases in near-saturation conditions. *Journal of Marine Research*, *49*(3), 435–466.
Yeung, P. (2002). Lagrangian investigations of turbulence. *Annual Review of Fluid Mechanics*, *34*(1), 115–142.
Zappa, C. J., McGillis, W. R., Raymond, P. A., Edson, J. B., Hintsa, E. J., Zemmelink, H. J., et al. (2007). Environmental turbulent mixing controls on air-water gas exchange in marine and aquatic systems. *Geophysical Research Letters*, *34*, L10601. https://doi.org/10.1029/2006GL028790
Zhao, D., & Toba, Y. (2001). Dependence of whitecap coverage on wind and wind-wave properties. *Journal of Oceanography*, *57*(5), 603–616.
Zhao, D., Toba, Y., Suzuki, Y., & Komori, S. (2003). Effect of wind waves on air–sea gas exchange: Proposal of an overall CO_2 transfer velocity formula as a function of breaking-wave parameter. *Tellus B*, *55*(2), 478–487.
Zilitinkevich, S., Elperin, T., Kleeorin, N., Rogachevskii, I., Esau, I., Mauritsen, T., & Miles, M. (2008). Turbulence energetics in stably stratified geophysical flows: Strong and weak mixing regimes. *Quarterly Journal of the Royal Meteorological Society*, *134*(633), 793–799.